

Article

Reducing of Bend Scour by Setting Spurs in a Curved Channel

Dong-Sin Shih ^{1,*}  and Tzu-Yi Lai ²

¹ Department of Civil Engineering, National Chiao Tung University, Hsinchu 30010, Taiwan

² Department of Civil Engineering, National Chung Hsing University, Taichung 40227, Taiwan; eg09123love@gmail.com

* Correspondence: dsshih@nctu.edu.tw; Tel.: +886-3-5731917

Received: 2 April 2020; Accepted: 7 May 2020; Published: 10 May 2020



Abstract: In Taiwan, the rivers not only are fast-flowing with high discharge, but they badly erode their beds during the typhoon seasons. In addition, erosion on the concave bank in a meandering channel is the primary cause of levee break. Therefore, the study conducted a down-scale experiment on erosion induced by oblique flow in a laboratory. It was similar to number 27–34 cross sections of the Fengshan river of Hsinchu County, Taiwan. The region was chosen because there are some special attacking angles of water flow and historical precedents of levee break. The study adopted the discharges of return periods of 10 and 20 years and measured the flow field by laser doppler velocimetry (LDV). Then the protective effects with different spur types were examined. The results indicate that increasing velocity induces side erosion when the flow impacts with the adjacent angle on the concave bank. However, the decreasing of velocity causes deposition of sediment on the concave bank. Furthermore, based on the vertical velocity profile of water flow, a higher flow rate is measured in the downstream on the concave bank. After the spurs are installed, the velocity at the spurs in the downstream is reduced, and the cross section with the larger velocity is moved to upstream. In addition, after setting the spurs, the reduction rates in volume of scour are 7.97% of a 10 year return period and 4.65% of a 20 year return period, respectively. That demonstrates the scour is effectively reduced as long as the spurs are set. Although the erosion mitigation rate and protection effect are decreased when the velocity is high, there is still a good protection effect at the bank. The setting of spurs has the following effects: First, the maximum scour depth generates in the front spur, while the maximum scour position keeps away from the bank. Then, the overall flow rate can be reduced to approximately 35%–40% comparing with the original flow field. Lastly, the spur on the slope of 1/30 degrees demonstrated the best function of stretching the distance from the embankment.

Keywords: spur; erosion; concave bank; convex bank; laser doppler velocimetry (LDV)

1. Introduction

Due to the steep terrain and the heavy rainfall, the rivers in Taiwan are fast-flowing with high discharge. Many steep slope watersheds are severely eroded by rivers during the typhoon seasons because of the loose soils. Thus, sediment concentration and riverbed erosion are always critical issues which must be faced. In addition, the toe scour problem, especially in river bends and hydraulic structures, is very common in Taiwan [1]. Bank erosion is induced by the strong flows with the large amount of suspended sediment. Sometimes it even causes serious damage both on bank and hydraulic structures. In many cases of the broken bank, the concave bank is significantly eroded from the severe oblique impact of the flood [2]. During the past decade in Taiwan, the Kanding bank in Zhonggang River, was damaged by Typhoon Sinlaku (2008); the townships of Linbian and Jiadong in Pingtung

County suffered serious floods after the bank of the Linbian river was broken by Typhoon Morakot (2009); several banks were damaged with severe floods in Taoyuan City by extremely heavy rain on 11 June 2012; the extremely heavy rain on 16 June 2017, resulted in the destruction of the river bank when the fast and high discharge flowed into farmlands, which caused enormous loss of rice because of the broken bank in TaChu, Changhua County, etc. Most of the stream flows in Taiwan are winding and twisted due to the erosion and sediment concentration, and tend to cause river bank destruction [3].

Oblique flow is a relatively simple non-uniform flow. As the flow encounters a corner it deflects obliquely from the alignment of the channel. Flow deflection occurred on the upstream owing to a reduction in the velocity of channel. The deflection was enhanced within the channel, in which the longitudinal velocity was gradually accelerated [2]. The oblique flow was generated by the flows smashing against an oblique angle on the concave bank; thereby sediment concentration was deposited on the convex bank. Thus, the stream flows were changed by the impact of oblique flow and had caused severe toe scour on the river embankment [4,5]. The nearer to downstream, the wider the range of the scour was where the concave bank scours occurred [6]. In addition, there was a good consistency in the range of the scour. In general, the form of river erosion was closely related to the flow velocity and its launching flow velocity [7,8]. It can be further elaborated that the maximum scour depth was generated when channel flow reached the critical launching flow velocity for entrainment of bed sediment [9].

To further analyze the scour on the concave bank in a curved channel, the study carried out a down-scale experiment to scrutinize erosion at a curved riverbed, observing the impact of oblique flows and the scouring variation at ground sill. Generally, in river management, the protection, restoration of stability, and natural function of rivers have become the most important issues in recent years [10]. River stability relies on some work to protect a river within existing stable conditions. The organized spur protection, stream flow controlling, side wall scour prevention and changing flow directions are commonly used to protect the concave bank [11]. In addition, extensive research has been done in order to understand the scour mechanism and to develop proper protection techniques [12,13]. By means of setting the outer bank footing protruding in the flow with horizontal foundation, the maximum scour reduced more than 40% with proper placement [14]. Another effective strategy which is explored to protect the bank from scouring is the use of submerged vanes [15,16]. The flow and its sediment transports were diverted in a more stream-lined way by placing the vanes in an eroding bank with an angle of attack [17]. Finally, it prevented scour directly adjacent to the bank and results in the deposition of sediment at the eroding bank. For further application, a riprap design in which heavy and large blocks, individually set by mechanical methods, were utilized as proposed in [18]. It provided a stable lining to lower the scouring by channel water. Some of the methods have been practiced successfully, however, not all these methods are suitable for every site condition. Among the above methods, setting the apron and spur are the common and readily realized strategies in the engineering method of toe protection works.

In real practice, the method of constructing spurs is particularly common and appropriate in Taiwan for bank protection. The spur is a transverse structure built at the central portion of the river. Its function is to decelerate the flow velocity as well as decrease the sediment recruitment so that it can successfully protect the bank. By causing redirection of flows, the spurs prevent the dikes from the direct impact of flows. It can drain the river along the desired course to reduce the concentration of flow at the point of attack [19]. Open-channel flume experiments were conducted with a rectangular spur dike for focusing on turbulent flow measurements [20]. The measurements showed that the flow around the spur dike was characterized by highly complex flow phenomena [21,22], such as horseshoe vortices, shear layers, and secondary flows [23,24]. As the experiment demonstrated, the flow pattern at the free surface could be accessed in numerical simulations. The mechanism of spur protectors and dike scours behaviour were similar to abutment scours in local scours [25]. Basically, the local scour could be further classified into clear-water scour and live-bed scour [26].

As stated above, fast-flowing rivers in Taiwan lead to the footing erosion of hydraulic constructions constantly, especially in the concave side. In most cases of broken bank, the scouring mainly occurs in a curved channel, which is usually induced by oblique flows. Thus, this study conducts a down-scale experiment with a curved channel in a laboratory to simulate the before and after profiles of riverbed scour, toe erosion at river bends and flows around the spurs, to evaluate the effect of protection work. The results could benefit different protection works on hydraulic structures and their feasibility. Therefore, Section 1 of this study introduces the background and objectives of this study. Section 2 gives an overall presentation of experiment design and setting. To reduce the bend erosion, a down-scale experiment is designed on erosion induced by oblique flow in a laboratory. The results of the experiment are presented in Section 3. This section is divided into three parts to discuss respectively: (1) the bend erosions with/without spur protection of 10 and 20 years, (2) the flow field with/without spur protection, and (3) an overall comparison. In the Conclusion section, setting spurs is emphasized as successful protection work and increased slope tends to effectively lower the scour.

2. Design and Setting of Experiments

The study was conducted as a small-scaled experiment in the laboratory which was similar to number 27–34 cross sections of the Fengshan river of Hsinchu County. The site was selected because the study area had a special angle of attack of the flow, and there were many drastic cases of broken banks in the past few years. Since 2001, the Fengshan river has been damaged by Typhoon Nari. High tides and flash floods caused the banks to suddenly break, and resulted in inundation of the low-lying areas. After that, Typhoon Matsa (2005), Krosa (2007), Sinlaku (2008), Jangmi (2008) and Morakot (2009) also destroyed the protection of hydraulic structures in the Fengshan river. There once was serious destruction of its banks, which was made by Typhoon Saola in July 2012. The bank was broken, so the flood leaked out and surged from a crack on the left bank. The severe floods were generated along the left bank including the river shoreline to Yimin bridge.

To reduce the bend erosion, the experiment is designed based on the similarity law of watershed, with a glass flume (1:280 scale). The experiments were performed in a 12.0 m long, 0.5 m wide, and 0.5 m deep laboratory flume with a glass sidewall. The working length of the flume which represented the mobile bed zone was 1.0 m, selected to sufficiently guarantee full scour development without any geometrical interference. In the flume, the channel slope is 0.001 with a 30° angle of attack, as shown in Figure 1. The soil in this experimental movable bed is hypothesized as uniform sediment which is extracted from a field sample and dried at 105 °C (24 h is usually sufficient). The soil of median diameter (D_{50}) is 1.27 mm and 16 cm in thickness, and the ratio of D_{84} and D_{16} is 1.1, within the range of uniform sand. Although the soil used in this experimental movable bed is hypothesized as uniform gravel, the value is determined not only by the range of down-scaling estimations but to its the best matching scour depth of in-situ measurement. It is noted that the particle size has been verified by the scour experiments which were conducted with different particle size tests (in the flood recurrence of 20 years). Therefore, the experimental design will be closer to the on-site scouring situation. Then the eroding test is exploited in the flood recurrence interval of 10 and 20 years respectively. An instrument that utilizes laser doppler velocimetry (LDV), measures the flow field. The detailed equipment this study used are listed as following (right-to-left manner) as shown in Figure 2: The PowerSight module is a generator of light which includes solid state lasers together with transmitting and receiving optics. The PDM module is for the data conversion. The PDPA probe performs as a color filter. The Flowsizer software is utilized for all data accessing and processing.

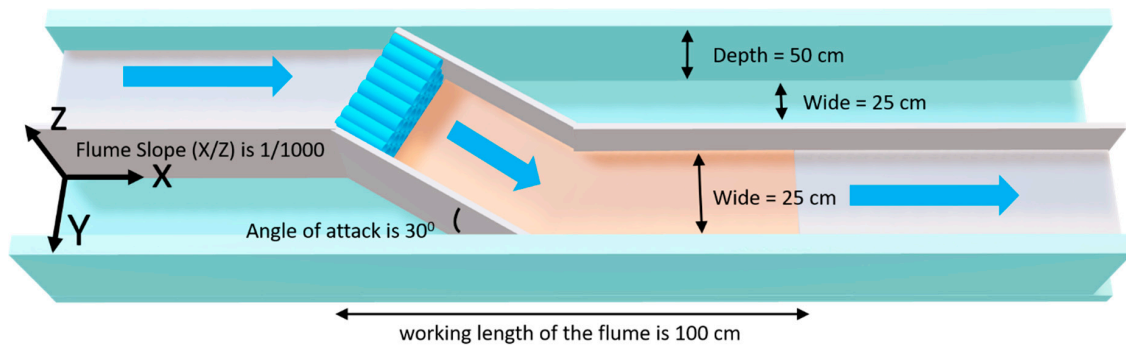


Figure 1. Sketch map of experimental channel (not to scale).

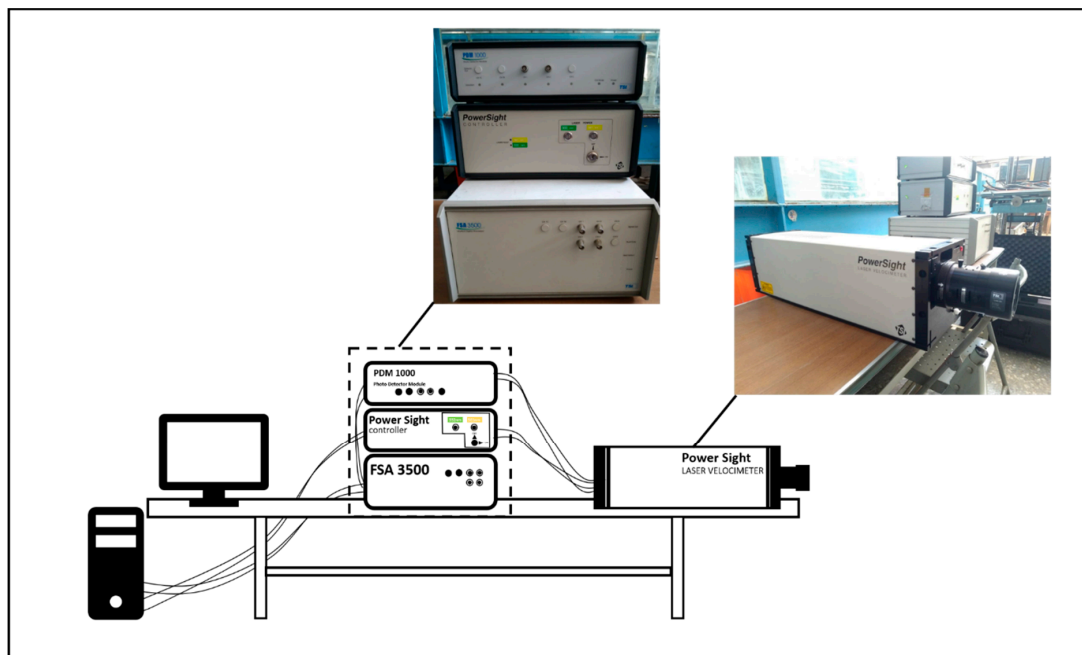


Figure 2. Laser doppler velocimetry (LDV) measurement.

The study finds that the erosion at the riverbed for four hours will be stabilized. Therefore, a set of initial conditions is used; the flood volume of 20 years (return periods) is used to conduct clear-water scour lasting for 5 h. The sands are spread out uniformly at the movable bed to ensure the consistent initial condition in every experiment. Furthermore, the method of protection the study utilized is two wooden spurs which are physically placed consecutively. The length, width and thickness are 4 and 6 cm of a spur. The intervals between two spurs is 5 cm. Both of them must protrude from the soil for 0.5 cm as shown in Figure 3. The ratio of D_g/L_g , where D_g is the distance between two spurs and L_g represents the length of the spur, was between 1.5 and 2.0 as a concave bank [20]. For our case, the D_g/L_g in this study is assigned as 1.67 on the channel. In addition, different controlled variables are set in the study such as various recurrence intervals of flood volume. All variables are utilized to conduct the experiments of the impact of oblique flow. The riverbed with uniform-height silt is also exploited to complete the erosion experiments. The results are conducive to understanding of erosion and flow direction, which can be further applied to the spur protections for river embankment.

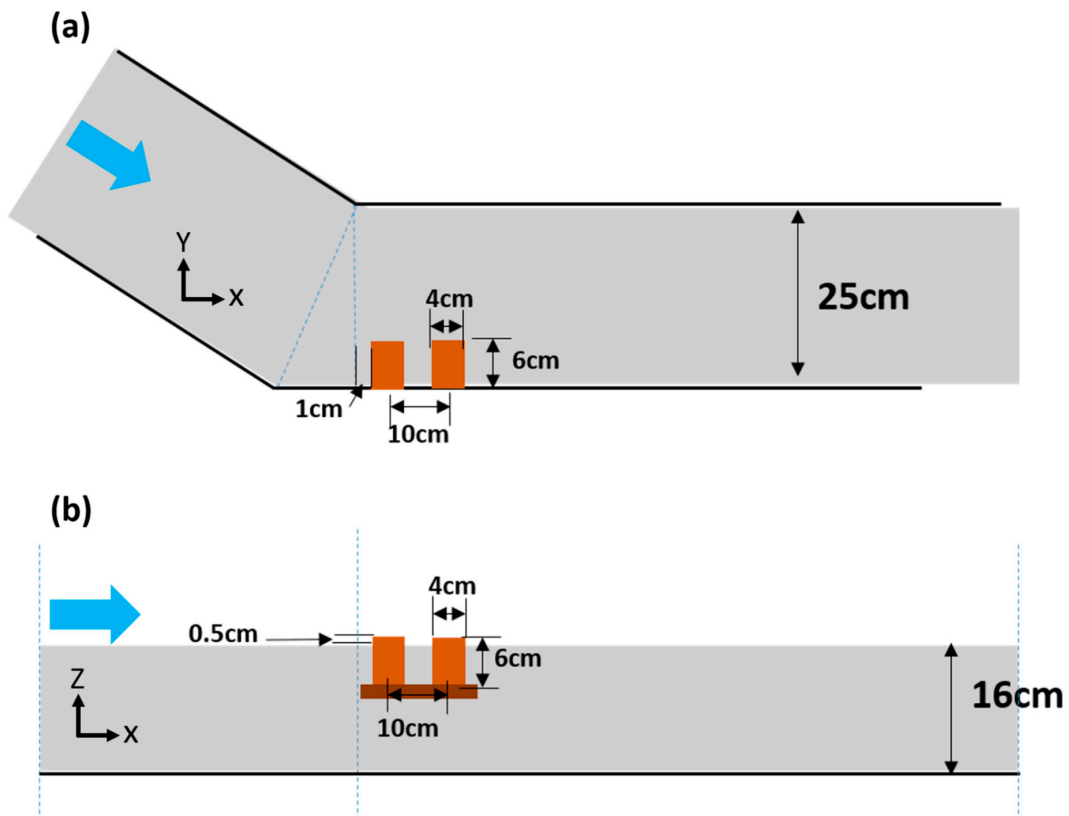


Figure 3. Spur (a) top view, and (b) side view.

The conditions of the experiment conducted in this study are presented in Table 1. A comparison of bend erosion without protection and bend erosion on two slopes (horizontal, 1/30) with spur protection is performed. The recurrence intervals of flooding for 10 and 20 years are utilized. Then the difference of elevation is charted and analyzed by the subtraction between two sets of data respectively: the bend erosion with spur protection and non-spur protection. Moreover, by using LDV, the estimation of the flow field on sections S1–S11 (total of 11 sections) are examined to measure surface flow velocities. The mean surface-velocities are analyzed by each interval point of 1 cm among 11 sections, a total of 25 points. Every point is evaluated with front, middle and back ($Y = 2$, $Y = 11$ and $Y = 23$) on each section to obtain the velocities of vertical section. The details are shown in Figure 4.

Table 1. Setups of experiment.

No.	Flow Recurrence Period (years)	Slope (%)
1	Non-Spur Protection	—
2		
3		
4	Spur Protection	horizontal
5		
6		

The calculation of volume of retardation rate (V_{RR}) under different arrangements is shown in Equation (1). The erosive volume retardation (V_{ER}) is obtained by the maximum erosive depth, and the calculation method is presented in Equation (2). It should be noted that the result showed that the more significant the spur protection demonstrated, the larger the positive numerical value displayed.

$$V_{RR} = \frac{V_E - V_P}{V_E} \times 100\% \tag{1}$$

$$V_{ER} = \frac{D_E - D_{SP}}{D_E} \times 100\%, \quad (2)$$

where V_{RR} is volume of retardation rate expressed in percent (%), V_E is the volume of bend erosion without protection, V_P is the volume of bend erosion with spur protection, V_{ER} is the erosive volume of retardation (%), D_E is the maximum depth of bend erosion without protection, and D_{SP} is the maximum depth of bend erosion with spur protection.

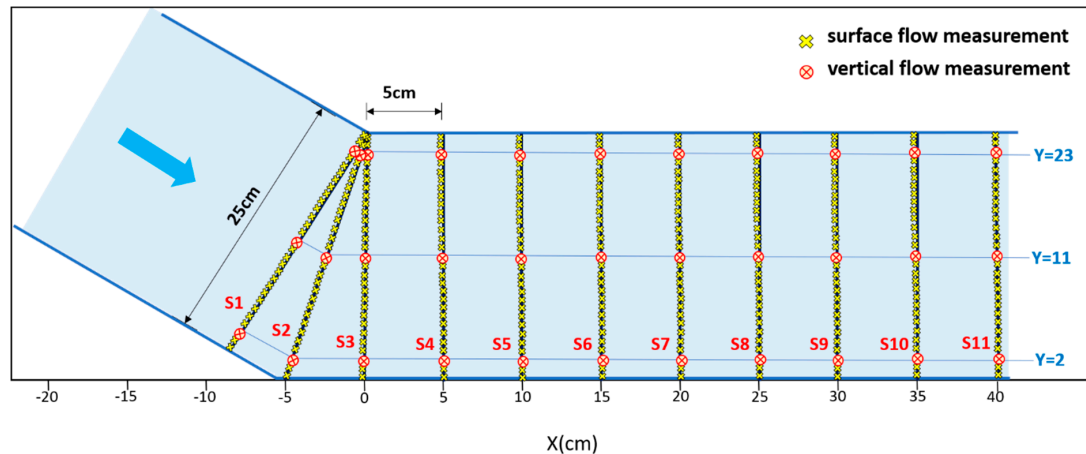


Figure 4. The flow field measurement of surface and vertical velocity.

3. Result and Discussion

3.1. Bend Erosions with/without Spur Protection

The results of bend erosion and flow field with and without spur protection, and with flood recurrence intervals of 10 and 20 years are shown in Figure 5. The results of bend erosion (without spur protection) indicate, on the concave bank, slight sediment accumulated before the stream flowed into the bend and afterwards a greater erosion generated at the bend. However, on the convex bank, little erosion occurred at the bend and then slight silt was deposited as shown in Figure 5a. In the bend, compared with the mechanism of non-spur protection, spur protection induced less sediment and slighter erosion at the first spur on the concave bank as shown in Figure 5b. The impact was erosion and sediment volume were both mitigated on the convex side. In addition, the sediment tended to move to the central part of the channel and accumulated there. Therefore, the phenomenon of the scouring mitigation in downstream and a change in the eroding position (near the spurs) were presented as the protective effect after the setting of spurs. Figure 5c further indicated a more significant variation of scour was revealed in in the 20 years discharge period rather than in the 10 years discharge period. On the concave bank, the sediment increased significantly before the bend as long as the flow increased. On the convex site, greater erosion occurred at the bend in comparison with the data in the 10 years discharge period. Then the sediment volume increased after the stream flowed into the bend. However, for the case of setting the spur, the results clearly showed the maximum erosive depth did not touch the outer bank, as shown on the portion of darkest red of Figure 5d. It meant that the maximum scouring position was pushing away from the original position. The minimization of erosion and the volume of deposited sediment was clearly presented on the convex bank. Overall, the spur protection can effectively alleviate both the erosion and deposition on the curved bend.

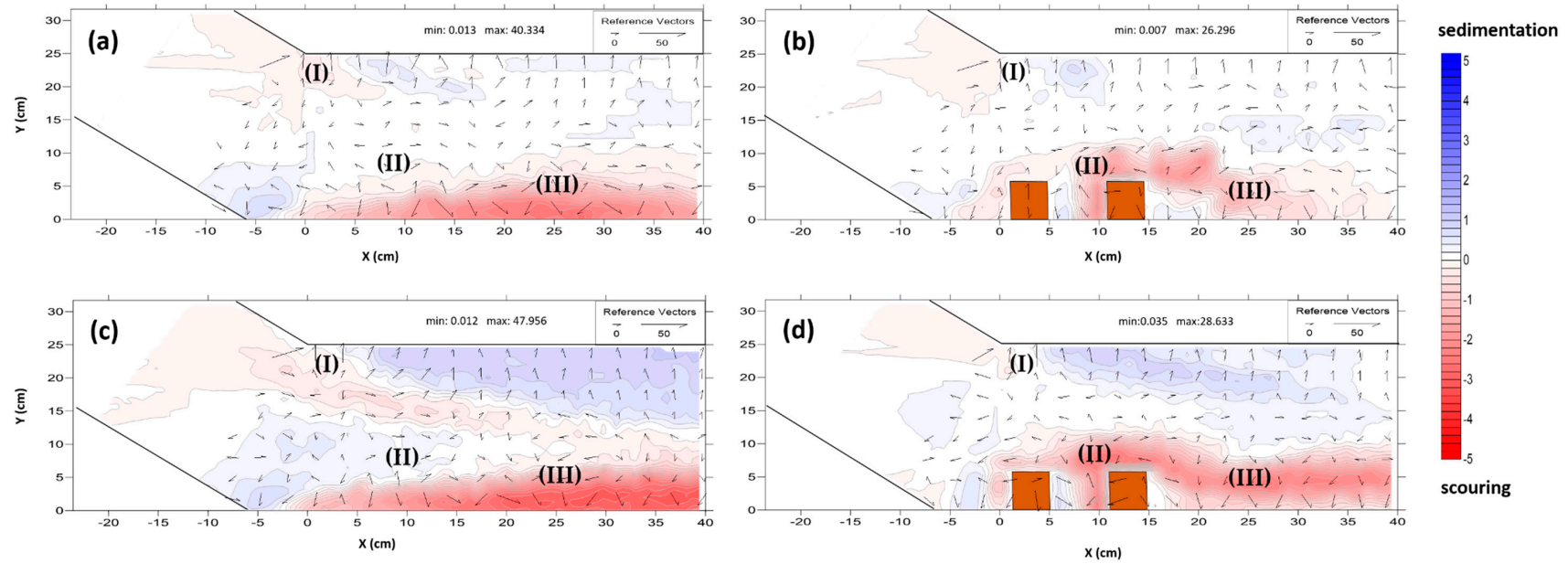


Figure 5. The scouring/sedimentation and velocity of (a) 10 years discharge period without spur protection, (b) 10 years with spur protection, (c) 20 years discharge period without spur protection and (d) 20 years discharge period with spur protection.

Flow fields from S1 to S11 were measured by LDV. The mean surface-velocities were analyzed at each interval point of 1 cm among 11 sections, and its maximum and minimum values are shown in Figure 5. In a flood return period of 10 years, for the Figure 5a, the result shows the surface velocity is higher in the erosion area while it is slower in the deposition area. The maximum and minimum velocities are 40.334 cm/s and 0.0132 cm/s, which reveals the velocity was positively correlated with scour. After setting spur protection as shown on Figure 5b, the surface-velocity decelerated sharply to 26.296 cm/s (maximum velocity) because the spur protection successfully reduced the impact of erosion. Moreover, the erosion and deposition on the bank were also reduced. Therefore, the spur protection effectively mitigated the erosion on the concave bank as well as the sediment on the convex bank. In the flood recurrence interval of 20 years, Figure 5c shows the greatest velocity is on the concave bank when the flow volume increased. It also represents the severe impact of erosion that occurred. Moreover, from the perspective of the convex side, the sedimentation in the 20 years recurrence interval was more serious than in the 10 years interval. The maximum velocity rose by 47.956 cm/s, which served to enhance erosion and deposition. However, setting of spurs can mitigate both the surface velocity and erosion as shown in Figure 5d. Erosion was still generated at these two spurs. The overall surface velocity reduced to 28.63 cm/s, which indicated the impact of erosion was weakened successfully. From the above results, setting of spurs can effectively mitigate the scouring on the curved channel.

The study further took into account the flood recurrence interval of 10 years and 20 years to study the scouring with 1/30 spur slopes. The results are shown in Figure 6. In the flood return period of 10 years, Figure 6a shows that on the concave bank, there was little silt deposition before the stream flowed to the bend. It should be noted that, slight scouring was found at the first spur while large erosion generated at the second spur. On the convex bank, in contrast to Figure 5b, when the slope elevated to 1/30 degrees, the scouring hole narrowed at the second spur and the impact of erosion was also mitigated by the spurs. In short, as long as the slope was elevated, the scouring as well as the sediment was mitigated and reduced by the spurs in the downstream as the result showed. In the flood recurrence interval of 20 years, on the concave bank, there was an indication that the silt sediment and erosion at the two spurs both displayed a mitigating tendency. Similarly, there was an alleviating trend in erosion on the convex bank.

To estimate the flow field in the experimental domain by using LDV, the zone of severe soil erosion on the concave bank, its maximum surface velocity was 21.734 cm/s and the minimum surface velocity was 0.002 cm/s as shown in Figure 6a. There was a positive correlation between surface velocity and the impact of scouring. Compared with Figure 5b, the impact of erosion in Figure 6a was smaller at the spurs on a slope of 1/30 degree. The maximum surface velocity declined from 26.296 cm/s to 21.734 cm/s in the 10 years return period. Similarly, the minimum surface velocity fell from 0.035 cm/s to 0.002 cm/s. It is clear from the above result that as the slope elevates, the impact of erosion is reduced. For Figure 6b increasing the slope angle decreased the surface velocity. In this figure, the maximum surface velocity dropped from 47.956 cm/s to 27.039 cm/s. The contrast between Figure 6a,b shows that the maximum surface velocity raised from 21.734 cm/s to 27.039 cm/s when the discharge increased. Moreover, the spur on slope of 1/30 degrees lowered the effect of erosion and sediment on the concave and convex bank respectively. Even if the discharge of the 10 years return period increased to that of the 20 years return period, the spur remained its protection function.

In order to further discuss energy dispersion before/after setting spurs, the energy equation considering kinetic and potential energy was applied. Three scouring zones of the flow field, shown in Figure 5, are studied: (I) on the convex bank, (II) in front of spurs, and (III) along the sidewall on the downstream side of spurs. In the case of flood recurrence of 10 years, the erosion at the left convex bank without spur (zone I) shows that the maximum energy is 0.028 m while it decreases to 0.022 m after the spur was set. Total energy loss is 21.4%. In the case of flood recurrence of 20 years, the energy declines from 0.032 m to 0.025 m and its total energy dispersion is 21.7% after the horizontal slope spur is set. With respect to the slope changing, when the slope elevates to 1/30 degree, the energy losses are 22.6% and 22.7% for the 10 and 20 years recurrence periods, respectively. This reveals that

the spurs can effectively lower the impact on the left convex side of the bank. Based on the above results, even if the discharge of 10 years return increases to that of the 20 years return, there is a better ability of reducing the energy with 1/30 slopes of the spur than with the horizontal slope of the spur on the convex bank. However, the erosion becomes severe in front of the spur after the spur was set, as shown in zone II of Figure 5. The energy increases from 0.024 m to 0.030 m (increased by 26.0%) with the setting of horizontal spurs in the case of the 10 years recurrence period. The energy increases by 16.8% when the slope elevates to 1/30 degree. It means that excessive energy generates in the front of the spur, which induces the scouring. With respect to the sidewall in the downstream, the energy reduces by 36.3% and 34.95% for 10 and 20 years recurrent floods respectively, after the spurs were set. As the spur slope elevates to 1/30 degree, energy dispersion becomes 37.1% and 37.3% for 10 and 20 years recurrent floods respectively. It demonstrates that the sidewall in the downstream can be well protected from the spur, and the slope of 1/30 of spur provides better protection.

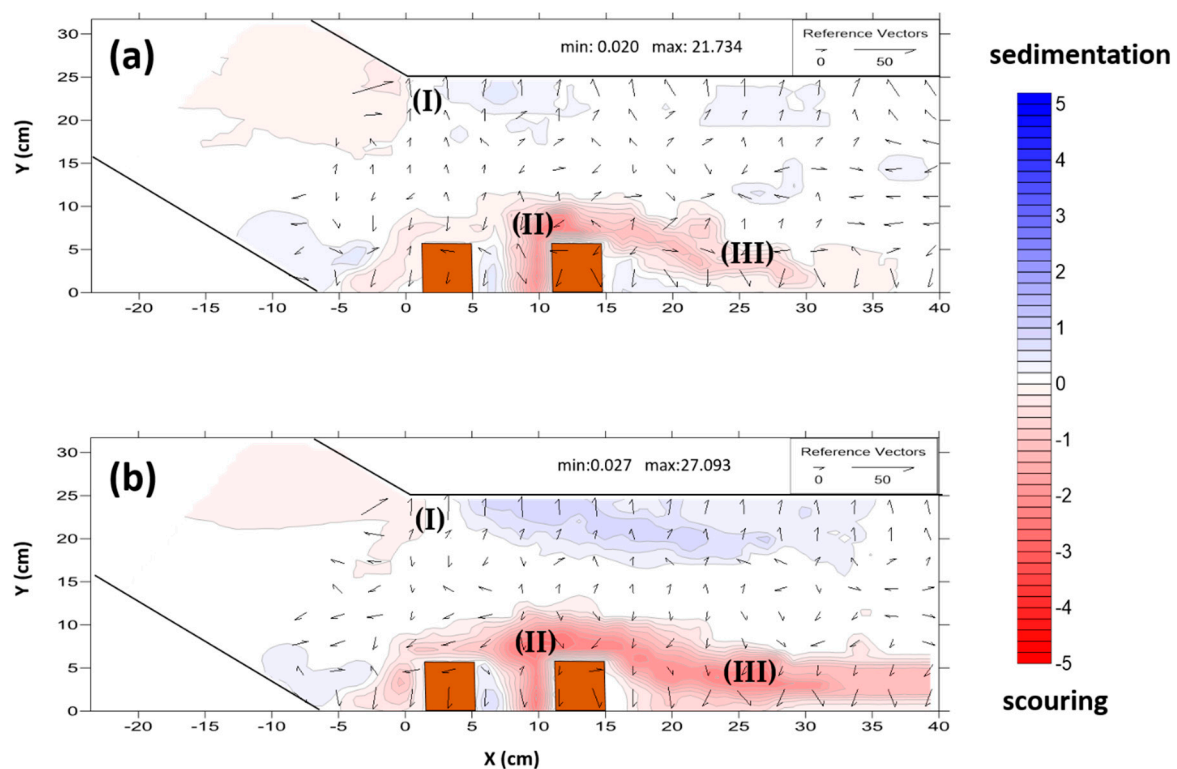


Figure 6. The scouring/sedimentation and velocity of 1/30 slope with spur (a) 10 year flood recurrence interval and (b) 20 year flood recurrence interval.

3.2. Flow Field with/without Spur Protection

Figure 7 shows vertical velocity of the flow field and its dimensionless scouring depth in the flood return period of 10 years with non-spur and spur protection. The velocity of the flow field on cross sections S1–S11 was examined by $Y = 2$, $Y = 11$ and $Y = 23$. The results showed that the velocity was proportional to the impact of erosion. For the case of non-spur protection in Figure 7a–c, the high velocities were presented at sections S8 and S10 defined in Figure 4, where the severe erosion also happened as for $Y = 2$. In addition, the erosion mainly occurred in the downstream because of the high velocities. As for $Y = 11$, there was a uniform and stable distribution in velocities in the middle drainage line. The high velocity generated the bend erosion in the upstream and it resulted in silt deposition with low velocity in the downstream as for $Y = 23$ in the sections S1–S5. The Figure 7d–f with spur protection revealed, when $Y = 2$, the main eroding position in the downstream shifted to the upstream so that the entire impact of erosion was mitigated by the spurs. Then the variation of

scour depth and flow velocity remained stable in the section of $Y = 11$. The lower scour depth but higher flow velocity were also the characteristics of $Y = 11$. As $Y = 23$, due to the decline of velocity and scour depth, the bend scour on the convex bank and the silt deposition in the downstream were both retarded after the spur protection had set.

Figure 8 shows the vertical velocity of the flow field in the flood recurrence interval of 20 years. In period of 20 years, compared with the Figure 8, when $Y = 2$ in Figure 7 with the increasing discharge, the high scour depth and velocity in the sections indicates severe erosion occurred in the middle-downstream. When $Y = 11$, the velocity remained stable and the scour depth increased slightly. The position of sections ($Y = 23$) was remote from the convex bank and it was taken as the area of silt deposition. The results showed there was erosion in the upstream and then the severe deposition occurred in the downstream because of the high velocities in S1–S4 and low velocities in S5–S11. Figure 8d–f further shows the spur protection achieved the effect of mitigation. The erosion was reduced because the main eroding position shifted from upstream to downstream as $Y = 2$. The variation of velocity and scour depth still maintained stability because of the spurs when $Y = 11$. The entire velocity declined and the impact of erosion also reduced. As $Y = 23$, the increased velocities in each section were found comparing with Figure 8a–c. It revealed the spurs alleviated the silt deposition on the convex bank.

Figure 9 revealed the velocity of experimental domain on 1/30 slope spur protections in different recurrence intervals of discharge. Figure 9a–c in the flood return period of 10 years revealed as $Y = 2$, the severe erosions and high velocities generated in S5, S6, and S7. The eroding of spur was presented in S5. As $Y = 11$, compared with Figure 7b, the velocities in Figure 9a–c slightly decreased with uniform distribution of velocity in each section. Then as $Y = 23$, the high velocity of flows caused the erosion at the bend and then generated the silt sediment in the middle-downstream with low velocity. In the return period of 20 years, Figure 9d–f displayed that the main eroding position in the downstream shifted to upstream, and the velocity in the main eroding area was reduced, which represented the enhancement of spur protection as $Y = 2$. The scour depth and velocity remained stable as $Y = 11$. Then comparing Figure 8d with Figure 8f, it revealed the entire velocity and scouring effect increased when $Y = 23$. In short, the result can be clearly seen that the bend scour on the convex side was retarded after the spur was set. And the overall velocity of the flow field was slight reduced.

The shear stress on the riverbed was also an important factor to evaluate the effect of spur protection. Figure 10 shows the shear stress of the flow field with flood recurrence intervals 10 and 20 years. Figure 10a reveals the dots in S3 and S4 had higher shear stress which meant the erosion was generated at the front of the spur as $Y = 2$. In addition, taking S4 as an example in Figure 10b, the shear stress of the dots was lower than the triangular point on the riverbed. It demonstrated the spurs can effectively lower the shear force as well as the impact of erosion. When $Y = 23$ in Figure 10c, the shear stress with spur was higher (dots) than the shear stress without spur (triangular points). It displayed that increasing of velocity resulted in reduction of the silt deposition after the spurs were set.

Comparing the shear stress of spur protection with non-protection, when the return period increased to 20 years, the shear stress increased as $Y = 2$ and 11, while it declined as $Y = 23$. It indicates the impact of erosion enhanced in the middle-upstream and the silt deposition increased in the downstream which was remote from the embankment. As $Y = 2$, the spur had no significant effect on protection when the flow velocity continued to accelerate because the two shear stresses had similar values. The distance between dots and triangular points became closer as the results presented. The increased velocity as well as the decreased silt deposition were due to the effect of spur protection as shown in $Y = 23$. In other words, the existence of the spur can accelerate the flow velocity whereas the sediment was reduced under higher velocity. Above all, it certainly protected the bend by pushing the power of scouring away from the embankment.

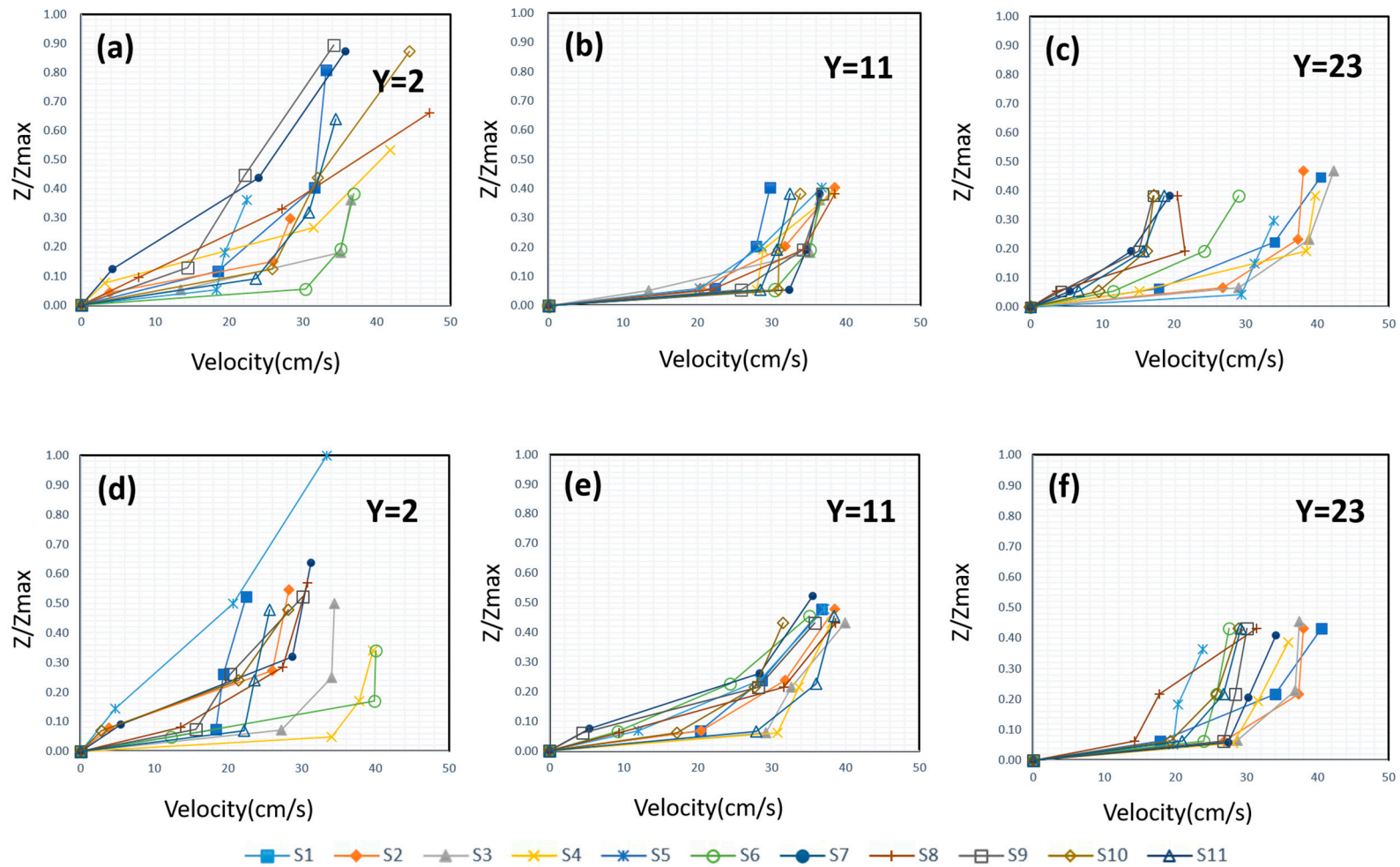


Figure 7. The sectional vertical velocity and its dimensionless scouring with (a–c) non-spur protection, and (d–f) spur protection in the flood return period of 10 years.

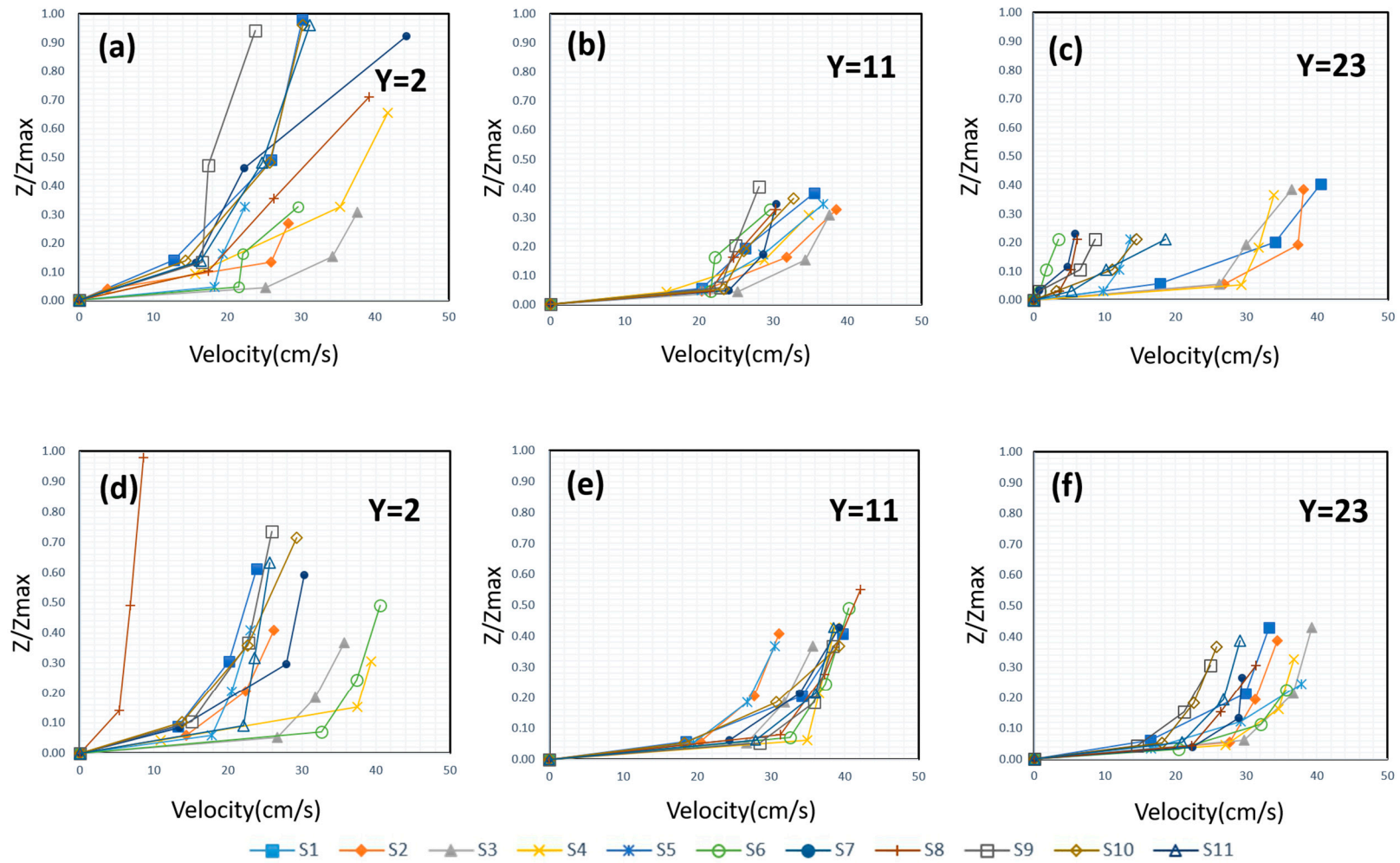


Figure 8. The sectional vertical velocity and its dimensionless scouring with (a–c) non-spur protection, and (d–f) spur protection in the flood return period of 20 years.

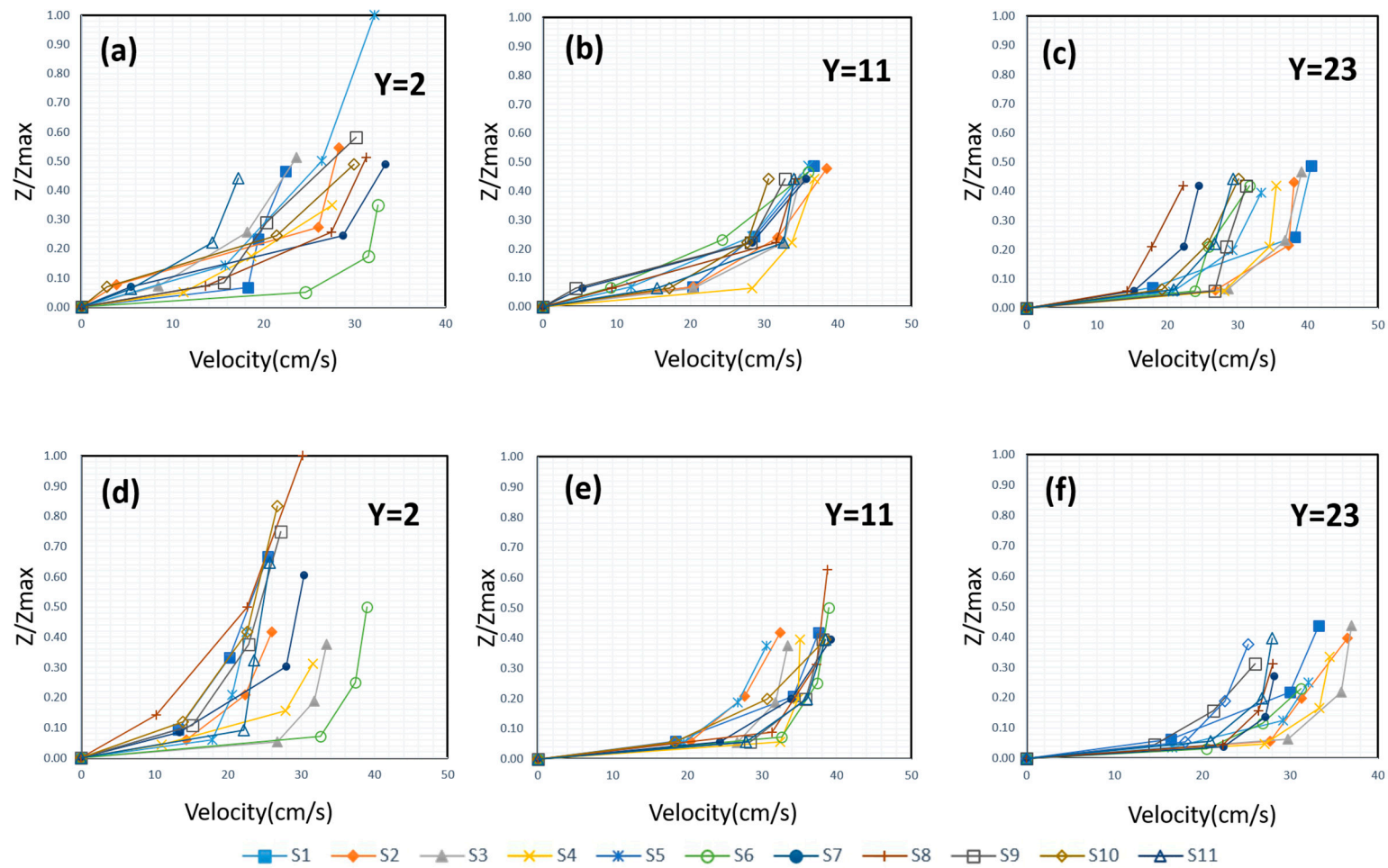


Figure 9. The sectional vertical velocity and its dimensionless scouring on 1/30 slope spur on flood recurrence interval of (a–c) for 10 years flood return period, and (d–f) for 20 years flood return period.

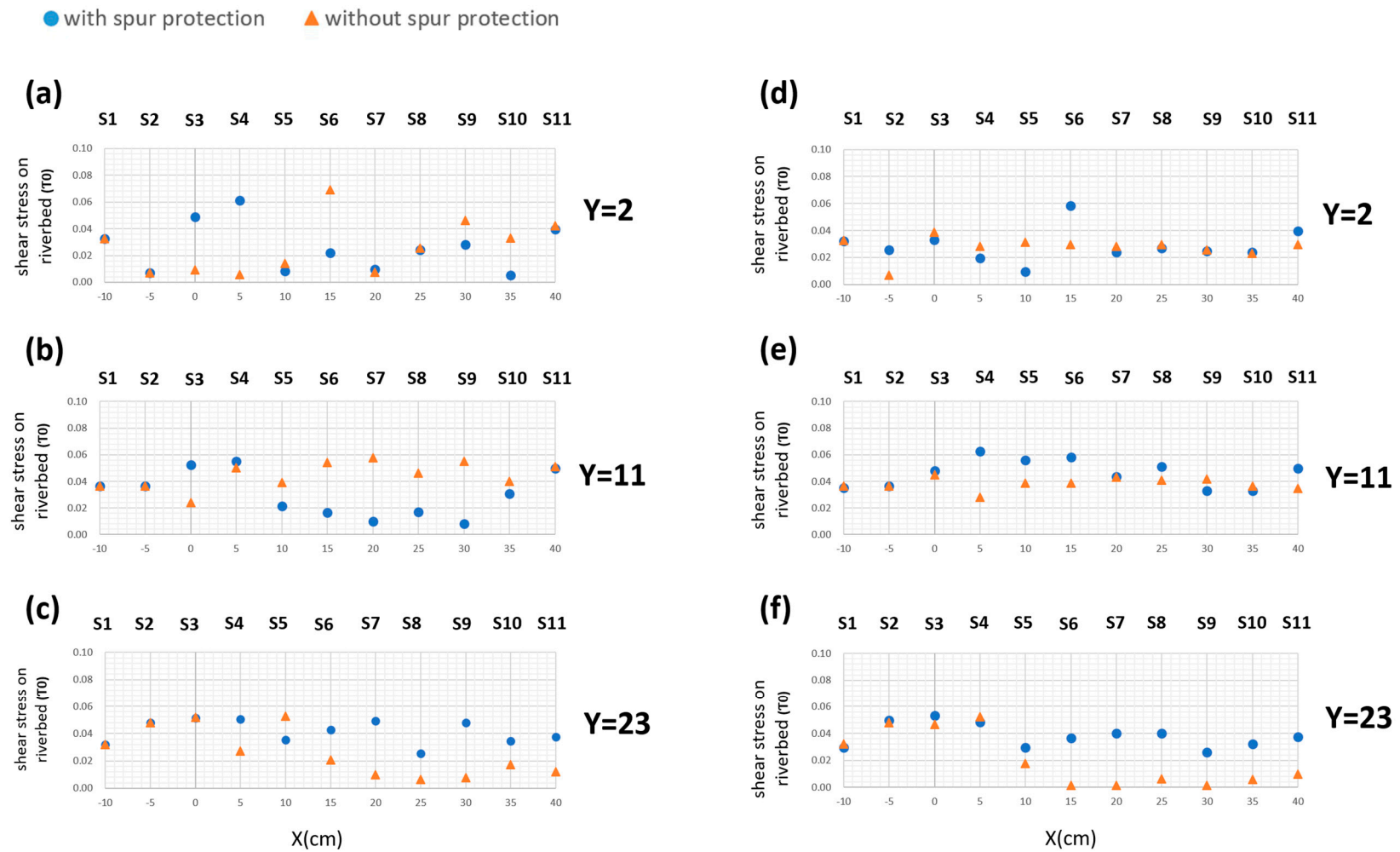


Figure 10. The distribution of shear stress of the river bed with flood recurrence interval is (a–c) 10 years, and (d–f) 20 years.

3.3. Overall Comparison

The volume of retardation rate (V_{RR}) was a comparative factor to evaluate the effect of spur protection. Table 2 lists the volume of retardation rate on the slope of horizontal and 1/30 with spur protection and non-spur protection. As Table 2 reveals the V_{RR} is 7.97% on the horizontal slope of spur in the 10 years flood recurrence interval while the value declined to 4.65% in the 20 years period. The two values are positive which means the river bank was well protected. The study further conducted experiments of a 1/30 slope spur for studying erosion. In the flood return period of 10 years, the erosive retardation rate was 7.94% on a horizontal slope, whereas it increased to 11.43% on the slope of 1/30. A similar ameliorated situation in the erosive retardation rate occurred in the return period of 20 years. Therefore, the result revealed the effect of spur protection on the slope of 1/30 was better than on the slope of horizontal degree, even though the high velocity generated and it indeed slightly lowered the effect of protection. As Table 2 also shows, on the slope of 1/30, the erosive retardation rate is 11.43% in the return period of 10 years; then the rate fell to 8.76% in the return period of 20 years. Although the effect of protection tended to be weakened to accompany with floods, there was still an obvious tendency that the protection of a spur could be enhanced.

Table 2. The volume retardation rate on the slope of horizontal and 1/30 with spur protection and normal bend scour (non-spur).

No.			Slope (%)	Volume after Erosion (cm ³)	Volume of Retardation Rate (%)
1	Non-Spur	10 year	—	1589.058	—
2	Protection	20 year	—	1770.834	—
3		10 year	horizontal	1462.963	7.97
4	Spur Protection	20 year	horizontal	1688.481	4.65
5		10 year	1/30	1407.427	11.43
6		20 year	1/30	1615.663	8.76

By using the value of the maximum erosive depth over the experimental domain, the erosive retardation in comparison with different return periods of discharge can be obtained as shown in Table 3. Table 3 shows the erosive retardation was 25.93% on the horizontal slope of spur in the flood recurrence interval of 10 years while the value declined to 21.88% in the period of 20 years. The two values were positive, which shows the effective protection of the spur. The drop in the erosive retardation revealed the effect of protection was slightly reduced. The spur protection on the slope of horizontal degree and 1/30 compared with the erosive retardation was also presented. In the flood recurrence interval of 10 years, the erosive retardation was 25.93% on the slope of horizontal degree, while it grew to 59.26% on the slope of 1/30. Similar rising situation in the erosive retardation rate occurred in the period of 20 years. Overall, according to above results, the effect of spur protection on the slope of 1/30 was also better than on the slope of horizontal degree, even though the high velocity weakened the effect of protection. In addition, the above result was consistent with the result of retardation rate which revealed there was a negative correlation between velocity and erosive retardation. Although the effect of spur protection slightly declined when the velocity accelerated, the bend with spur protection still mitigated the eroding and sediment effectively.

Table 3. The erosive retardation rate on the spur slope of horizontal and 1/30 with spur protection and normal bend scour (non-spur).

No.			Slope (%)	Maximum Scour Depth (cm)	Erosive Retardation (%)
1	Non-Spur	10 year	—	2.7	—
2	Protection	20 year	—	3.2	—
3		10 year	horizontal	2.0	25.93
4	Spur Protection	20 year	horizontal	2.5	21.88
5		10 year	1/30	1.1	59.26
6		20 year	1/30	2.0	37.50

In Figure 11, the comparison of the maximum scour depth with the sections is presented. Experimental results indicate the variation of maximum scour depth had an increasing trend (2.6 cm (cross dots line) to 3.2 cm (triangular dots line)) when the return period of 10 years increased to 20 years. However, the maximum scour depth declined sharply for the cases with spur protection. The most serious eroding occurred at the spur and the value was merely 2.4 cm (rectangular dots line). The value 2.4 cm, was still smaller than the maximum scour depth (2.6 cm (cross dots line)) on the bend without spur. In the periods of 20 years, the effect of spur protection was still impressive because the scour depth of bend with spur-protection was 2.9 cm (cross dots line) which was smaller than without spur-protection, 3.2 cm (triangular dots line). After further comparison the protection by setting spur with two slopes (horizontal and 1/30), there was no significant difference in results between the spur slope of 1/30 and the horizontal with the discharge of 10 years recurrence interval based on Figure 11, because the maximum scour depths were both 2.4 cm on these two slopes. However, as the slope of horizontal degree elevated to 1/30, the maximum scour depth went down from 2.9 cm (cross dots line) to 2.7 cm (dots line) in the 20 years period. It demonstrated that the spur on the slope of 1/30 had more protective effect than the slope of horizontal degree. Moreover, it was notable that the maximum scour depth all occurred near the spur. The combined results of maximum scour depth and its retardation rate reflected that the increased slope tended to lower the scour successfully. The above discussions have confirmed the spur protection can effectively mitigate the eroding and sediment.

Lastly, the study further evaluated whether the riverbank in the downstream can be protected effectively by the spur. The variation of elevation along the channel was examined for obtaining the distances between the maximum scour position and the right embankment, shown in Figure 12. In a flood recurrence interval of 10 years, the maximum scouring just occurred on the right embankment before the spurs were set. However, the distance was around 7 cm and the maximum scour depth declined from 2.7 cm to 2 cm after the horizontal spur was constructed. In order to further check on the slope of 1/30, the distance was 8 cm, and the maximum scour depth decreased to 1.1 cm. The result demonstrated that the elevated slope is not only successfully declines the scour depth but also stretched the distance to protect the river dike. There was a similar tendency for the distances in flood recurrence interval of 20 years. The distance was 1 cm (triangular dots line) near the embankment without the spur protection. Then the distance stretched to 4 cm (diamond dots line) because of the construction of spur. The maximum scour depth dropped from 3.2 to 2.5 cm.

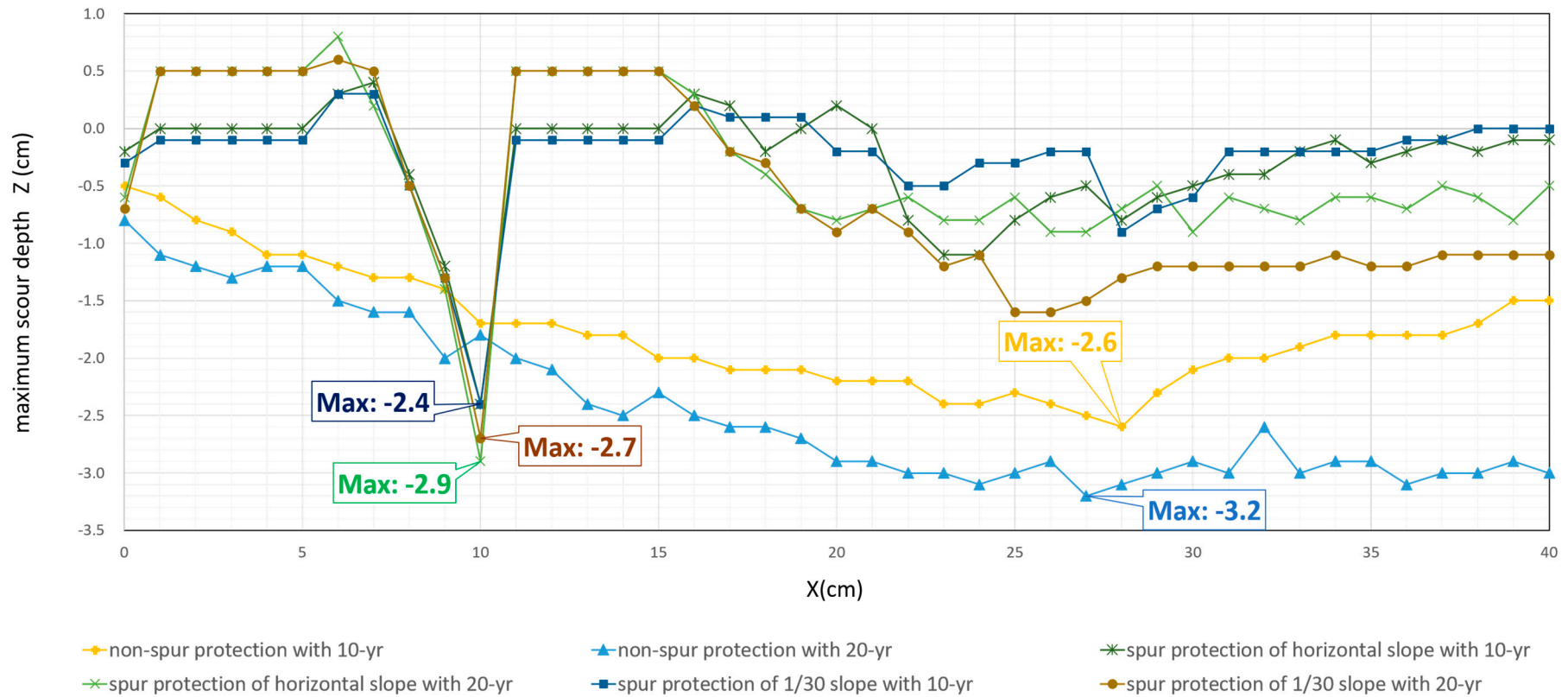


Figure 11. The maximum scour depth along the sections with spur and non-spur protections.

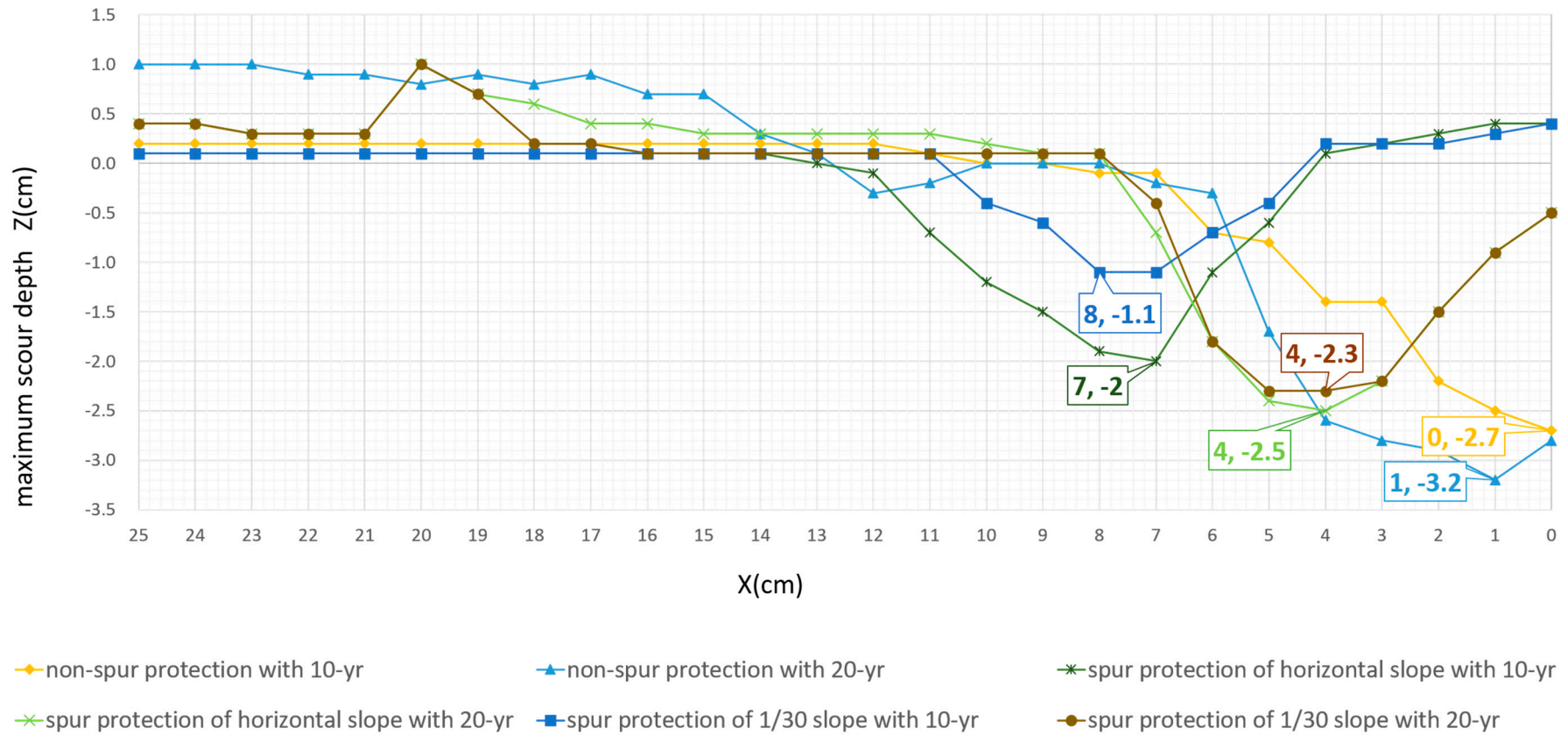


Figure 12. The maximum scour position of cross section with and without spur protections.

However, the spur on these two kinds of slopes had the same distances as 4 cm, which revealed it had limited effect on distance-extending when the discharge occurred for the period of 20 years. It demonstrated that the spur can effectively prevent the maximum scour position from nearing the embankment. In addition, the effect of spur protection was directly affected by the distances. As long as the distances between maximum scour position and the embankment stretched further, the effect of protection tend to be enhanced. In sum, all the results showed there still were some distances between the maximum scour position and embankment which showed that the spur remained the function of protection on the river bank.

4. Conclusions

The scouring problem, especially in riverbend and hydraulic structures, is a critical issue in Taiwan. Setting spurs as a protection is particularly common. The study conducts a down-scale experiment on erosion induced by oblique flow in a laboratory; the bend scour and spur protection are also drawn from the presented study. The soil of median diameter ($D_{50} = 1.27$ mm) with $1.1(\sqrt{d_{84}/d_{16}})$ standard deviation with uniform gravel is used in the experiments. The experiment result demonstrates that there is low velocity as measured at the general bend scouring, which also resulted in accumulation of sediment. However, the velocity accelerates when flows pass over the curved bend and the impact of toe scouring enhances. The maximum scour depth therefore generates near the side wall. As the experimental data reveals the bend scouring and sediment are mitigated effectively by the spur protection. In the flood recurrence interval of 10 and 20 years, the spurs still remain the effective means of protection even though higher discharges are suffered. In addition, with respect to the maximum scour depth, the spur structures successfully kept the entire scour positions a distance from the embankment to achieve the goal of protection. Based on the experiment of flow field, the maximum surface velocity decelerates sharply when the spurs are installed. It demonstrates the spur protection successfully reduces the impact of erosion and effectively mitigates the erosion on the concave bank as well as the sediment on the convex bank. Moreover, according to the vertical flow velocity profile, the higher velocity of sections (S3–S6) moves to upstream and distances itself from the bank. When the spur slope increases, the entire erosion tends to be mitigated as the data revealed. To conclude the results of maximum scour depth and its retardation rate, the increase of slope tends to lower the scour successfully. Especially, the spur on the slope of 1/30 demonstrates the best function of stretching the distance from the embankment. In short, the study has demonstrated that the scour along the sidewalls can be effectively reduced by setting spurs. The severe scouring will move in front of the spurs, while the maximum scour position keeps away from the bank. It reveals that the spurs can effectively lower the impact on the convex side, and provides a better ability of reducing the scouring with spurs with 1/30 slopes than with spurs with a horizontal slope.

Author Contributions: D.-S.S. conceived and designed the study, conducted the experiment, implemented data analysis, and wrote the paper. T.-Y.L. conducted the experiments and analyzed the data. All authors have read and agreed to the published version of the manuscript.

Funding: This research is funded by the Ministry of Science and Technology, Taiwan, under Grant no. MOST-108-2628-M-009-005.

Conflicts of Interest: The authors declare no conflict of interest.

References

1. Shih, D.S.; Yeh, G.T. Identified model parameterization, calibration, and validation of the physically distributed hydrological model WASH123D in Taiwan. *J. Hydrol. Eng.* **2011**, *16*, 126–136. [[CrossRef](#)]
2. Jensen, J.H.; Madsen, E.S.; Fredsøe, J. Oblique flow over dredged channels. II: Sediment transport and morphology. *J. Hydraul. Eng.* **1999**, *125*, 1190–1198. [[CrossRef](#)]
3. Hsu, T.W.; Shih, D.S.; Chen, W.J. Destructive flooding induced by broken embankments along Linbian Creek, Taiwan, during Typhoon Morakot. *J. Hydrol. Eng.* **2015**, *20*, 05014025. [[CrossRef](#)]

4. Blanckaert, K. Hydrodynamic processes in sharp meander bends and their morphological implications. *J. Geophys. Res.* **2011**, *116*, F01003. [[CrossRef](#)]
5. Blanckaert, K.; Graf, W.H. Momentum transport in sharp open-channel bends. *J. Hydraul. Eng.* **2004**, *130*, 186–198. [[CrossRef](#)]
6. Markham, A.J.; Thorne, C.R. Geomorphology of gravel-bed river bends. In *Dynamics of Gravel-Bed Rivers*; Billi, P., Hey, R.D., Thorne, C.R., Tacconi, P., Eds.; Wiley: Chichester, UK, 1992; pp. 433–456.
7. Melville, B.W.; Raudkivi, A.J. Flow characteristics in local scour at bridge piers. *J. Hydraul. Res.* **1977**, *15*, 373–380. [[CrossRef](#)]
8. Chiew, Y.M.; Melville, B.W. Local scour around bridge piers. *J. Hydraul. Res.* **1987**, *25*, 15–26. [[CrossRef](#)]
9. Melville, B.W.; Coleman, S.E. *Bridge Scour*; Water Resources Publications LLC: Lone Tree, CO, USA, 2000; 572p, ISBN 1887201181 (pbk.).
10. Lacey, G. Stable channels in alluvium. Paper4736, Minutes of the Proc. In *Institution of Civil Engineers*; William Clowes and Sons Ltd.: London, UK, 1930; Volume 229, pp. 259–292. [[CrossRef](#)]
11. Galay, V.J.; Yaremko, E.k.; Quazi, M.E. *River Bed Scour and Construction of Stone Riprap Protection in Sediment Transport in Gravel-Bed Rivers*; Thorne, C.R., Bathurst, J.C., Hey, R.D., Eds.; John Wiley & Sons, Inc.: New York, NY, USA, 1987; pp. 353–379.
12. Melville, B.W. Pier and abutment scour: Integrated approach. *J. Hydraul. Eng. ASCE* **1997**, *123*, 125–136. [[CrossRef](#)]
13. Thorne, C.R. *Velocity and Scour Prediction in River Bends*; Contract Report HL-93-1; US Army Engineer Waterways Experiment Station: Vicksburg, MS, USA, 1993; p. 66.
14. Roca, M.; Martín-Vide, J.P.; Blanckaert, K. Reduction of bend scour by an outer bank footing: Footing design and bed topography. *J. Hydraul. Eng.* **2007**, *133*, 139–147. [[CrossRef](#)]
15. Bhuiyan, F.; Hey, R.D.; Wormleaton, P.R. Bank-attached vanes for bank erosion control and restoration of river meanders. *J. Hydraul. Eng.* **2010**, *136*, 583–596. [[CrossRef](#)]
16. Ouyang, H.; Lu, C. Optimizing the spacing of submerged vanes across rivers for stream bank protection at channel bends. *J. Hydraul. Eng.* **2016**, *142*, 04016062. [[CrossRef](#)]
17. Chatley, H. Curvature effects in open channels. *Eng. Lond. Engl.* **1931**, *131*. [[CrossRef](#)]
18. Jafarnejad, M.; Franca, M.J.; Pfister, M.; Schleiss, A.J. Design of riverbank riprap using large, individually placed blocks. *J. Hydraul. Eng.* **2019**, *145*, 04019042. [[CrossRef](#)]
19. Chang, Y.L.; Hsieh, T.Y.; Chen, C.H.; Yang, J.C. Two-dimensional numerical investigation for short-and long-term effects of spur dikes on weighted usable area of *Rhinogobius candidianus* (Goby). *J. Hydrol. Eng.* **2013**, *139*, 1297–1303. [[CrossRef](#)]
20. Jeon, J.; Lee, J.Y.; Kang, S. Experimental Investigation of Three-Dimensional Flow Structure and Turbulent Flow Mechanisms Around a Nonsubmerged Spur Dike with a Low Length-to-Depth Ratio. *Water Resour. Res.* **2018**, *54*, 3530–3556. [[CrossRef](#)]
21. Blanckaert, K.; de Vriend, H.J. Secondary flow in sharp open-channel bends. *J. Fluid Mech.* **2004**, *498*, 353–380. [[CrossRef](#)]
22. Thorne, C.R.; Hey, R.D. Direct measurements of secondary currents at a river inflexion point. *Nature* **1979**, *280*, 226–228. [[CrossRef](#)]
23. Bathurst, J.C.; Thorne, C.R.; Hey, R.D. Direct measurements of secondary currents in river bends. *Nature* **1977**, *269*, 504–506. [[CrossRef](#)]
24. Bathurst, J.C.; Thorne, C.R.; Hey, R.D. Secondary flow and shear stress at river bends. *J. Hydraulic. Div. Am. Soc. Civ. Eng.* **1979**, *105*, 1277–1295.
25. Barbhuiya, A.K.; Dey, S. Local scour at abutments: A review. In *Adhana-Academy Proceedings in Engineering Sciences*; OCT: Toronto, ON, Canada, 2004; Volume 29, pp. 449–476. [[CrossRef](#)]
26. Chabert, J.; Engeldinger, P. *Etude des Affouillements Autour des Piles de Ponts*; Serie A; Laboratoire National d'Hydraulique: Chatou, France, 1956. (In French)

